Onion juice assisted green reduction of graphene oxide with tunable structural and optical properties: Effect of onion juice concentration and reaction temperature

Sumeet Kumar[1], Dipjyoti Bhorolua[1], Animesh K. Ojha[2], Ashok Kumar[1]*

[1]*Department of Physics, Tezpur University, Tezpur 784028 Assam, India*
[2]*Department of Physics, Motilal Nehru National Institute of Technology, Allahabad 211004, Uttar Pradesh, India*

*Corresponding author: Tel: (+91)-371-2275553; E-mail: ask@tezu.ernet.in

DOI: 10.5185/amlett.2019.2124
www.vbripress.com/aml

Abstract

In most of the studies, toxic and harmful reducing agents were used for the chemical reduction of graphene oxide (GO) and into reduced graphene oxide (rGO). Here, onion juice is used as a natural and green reducing agent for the reduction of GO into rGO. The effect of onion juice concentration and reaction temperature on the reduction ability of onion juice have been studied. The present synthesis approach avoids the use of toxic and harmful chemicals for reduction of GO. The mechanism of reduction of GO at various concentrations of onion juice is explained in terms of presence of cysteine in the onion juice as one of the chemical constituents. The X-ray diffraction (XRD) results revealed the high degree of reduction with superior quality. Transmission electron microscopy (TEM) images provide clear evidence for the formation of transparent and thin layers of graphene. We have extended our analysis to reveal the quality of rGO produced by onion juice assisted reduction of GO using D, G and 2D bands present in the Raman spectra. Moreover, we have discussed the role of onion juice concentration and reaction temperature on evolution of D and G bands and ID/IG ratio, which in turn tell the overall growth of graphene sheet. Fourier transforms infrared spectroscopy (FTIR) measurements also show significant degree of reduction of GO. The UV-Vis. absorption spectrum further confirms the ability of onion juice to reduce GO into rGO. The synthesized product shows good dispersibility in aqueous solvent. Thus, the present report provides a green and facile approach for the synthesis of graphene derivatives with enormous potential.

Keywords: Green reduction of GO, onion juice concentration, reaction temperature, degree of reduction.

Introduction

The increased attention in the development of carbon-based nanomaterials has opened a new possibility for the fabrication of advanced functional materials. Among them, graphene has emerged as a novel material due to their outstanding physical and chemical properties [**1**]. The remarkable characteristics of graphene have led the development of new area in the field of nanoscience and technology-based research. Since its discovery in 2004 [**2**], the synthesis of graphene has been one of the hottest areas in scientific community to explore their prospective applications in various fields e.g. energy storages, sensors, catalysis and optoelectronics [**3-5**].

Among the existing methods for the production of graphene, solution based chemical reduction route of GO offers simple and controlled synthesis of graphene on industrial scale. In solution based chemical reduction, GO is mostly reduced by highly toxic reducing agents such as hydrazine derivatives [**6**], ethylenediamine [**7**], hydroquinone [**8**] and sodium borohydrate [**9**] etc. The presence of the poisonous agents in these reducing agents put harmful effects towards ecological systems and further it also restricts their use in various areas. Moreover, the handling of these risky reducing agents is also a big hurdle and it also makes the entire synthesis process relatively costly. The above mentioned issues may nicely be addressed using natural reducing agents instead of chemical one. Many efforts have already been made by the scientific community towards green reduction of GO by natural products such as green tea [**10**] wild carrot root [**11**], leaf extracts [**12**], vitamin C [**13**], reducing sugar [**14**], glucose [**15**], cellulose [**16**], lemon juice, vinegar [**17**] and bacteria [**18**]. The main straightforward goal of any reduction protocol is to produce graphene like structure by reducing GO into rGO. However, in most of the cases, either an additional stabilizer with specific atmosphere is needed or the quality of final product is poor (exhibited highly agglomerated morphology). Therefore, the development of new low-cost green reducing agents for efficient reduction of GO into rGO at large scale is still highly desirable especially, which show solubility in water.

Taking advantage of reported literatures into account, herein, we present a facile and green novel approach to produce rGO through reduction of GO using onion juice. The change of the color of reaction mixture of GO from brown to black during synthesis confirms the removal of oxygen containing groups into rGO and signify the reduction efficiency of the present approach. The present approach demonstrates several unique features over the earlier reported strategies, which makes it relatively attractive for large scale production of rGO for practical applications: (i) the whole reduction process is environmental friendly, and no synthetic chemical is used (ii) it is relatively cheap and safe and does not need any external stabilizer or specific atmosphere (iii) it does not have a complex procedure and (iv) no hazardous waste is generated. The obtained rGO is characterized by different analytical and spectroscopic techniques. The transformation of GO into rGO using onion juice is clearly observed.

Experimental

Synthesis

GO was prepared by oxidizing the graphite powder in a mixture of concentrated sulfuric acid and phosphoric acid using $KMnO_4$ as reported previously [**19**] and demonstrated by Tour [**20**]. The onion juice was extracted from onion (red color) directly. In a typical experiment, 50 mg GO was added in 50 ml DI water and sonicated for 30 min. Thereafter, onion juice (0.5, 1.5, 3, 5 and 10 ml) was added to the colloidal solution of GO and stirred it for 2 hours (h) at room temperature and in an open atmosphere. Thereafter, the resultant solution was transferred into a Teflon lined autoclave for hydrothermal treatment at 150 ^{0}C for 12 h. Then, the solution was cool to room temperature. Subsequently, the resultant rGO was collected by filtration, washing with DI water followed by drying at 60^{0}C. To see the effect of reaction temperature on reduction ability of onion juice, another sample composed of GO and onion juice was also prepared via same method at 65^{0}C instead of room temperature. The samples rGO30_0.5, rGO30_1.5, rGO30_3, rGO30_5, rGO30_10 are named as S1, S2, S3, S4 and S5, respectively. The sample synthesized at 65^{0}C (rGO65_3) is named as S6. The schematic diagram of the synthesis procedure is presented in **Fig. 1**.

Characterization

To obtain the crystalline structure, reduction level and stacking of number of layers, the synthesized rGO samples were characterized by XRD, TEM, Raman, FTIR and UV-vis. spectroscopy. XRD spectrum was recorded on a Bruker Advance D8 diffractometer equipped Cu Ka radiation (λ=0.15406 nm). TEM images were obtained using JEOL JEM 2100 at 200 kV acceleration voltages. Raman spectra were taken using Renishaw Raman spectrometer (Renishaw, Wotton-under-Edge, UK) using 514.5 nm argon ion laser as an excitation source. FTIR spectra were recorded on a PerkinElmer Spectrum 100 spectrometer. UV-Vis. absorbance spectra of the water soluble rGO suspension were recorded using Shimadzu UV-2450.

Results and discussion

Onion juice assisted reduction mechanism of GO

The reduction mechanism of GO using onion juice could be explained using the essential amino acids (cysteine, leucine, tyrosine, lysine, threonine, valine, histidine etc.), sugars (sucrose, glucose, fructose, raffinose) and mineral elements (Na, K, Ca, Mg, Cu, Zn, Fe) present as

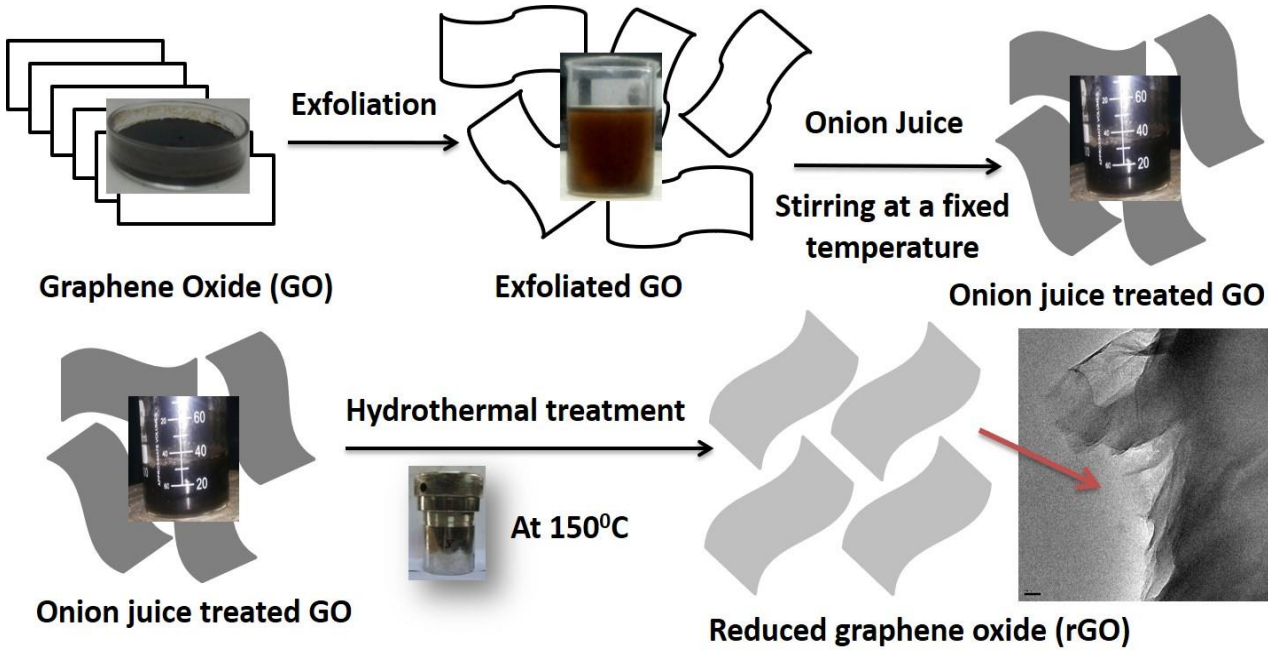

Fig. 1. Schematic diagram for synthesis of rGO using onion juice.

chemical constituents in the onion juice [**21**]. The reduction of GO using amino acids [**13, 22-24**], sugars [**14-16**] and metals [**25-27**] has already been reported. Most importantly, the onion juice contains six derivatives of cysteine, which are referred as antioxidants. It is reported that the antioxidants behave like as reducing agents for their intriguing ability of donating a single electron or hydrogen atom for reduction [**21**]. It should be noted that antioxidants are reducing agent but not all reducing agents could be antioxidants. It is reported that the antioxidant capacity of cysteine derivatives is increased after boiling [**21**]. Thus, in the present work, the mixed solution of GO and onion juice was prepared at 65^0C under constant stirring before hydrothermal treatment to use maximum antioxidant capacity of cysteine derivatives for well reduction of GO. To compare the effect of heating on reduction ability of onion juice, the mixed solution of GO and onion juice was also prepared at room temperature under constant stirring before hydrothermal treatment. Finally, the results obtained in the present study revealed that the reduction ability of onion juice is increased after heating with improvement in the quality of GO. The obtained results agreed well with the results reported previously [**22-27**]. The reduction of GO using onion juice is believed due to the presence of cysteine derivatives in it and the possible reasons have been explained. The structure of different derivatives of cysteine present in onion juice has been shown in **Fig. 2**. Each of the structure of cysteine derivatives contains sulfur and amine group (NH_2), which may be responsible for the reduction of GO. The use of sulfur containing compounds allows de-epoxidation of GO more easily due to weaker C-S bond energy while the NH_2 donate electrons to the oxygen functionalities attached to the GO surface [**28, 29**]. It is already reported that the several kinds of sulfur containing compounds such as $NaHSO_3$, SO_2, $SOCl_2$, $Na_2S_2O_3$, and Na_2S can serve as efficient reducing agents [**28**]. There are also several reports on the reduction ability of amine group (NH_2)[**29, 30**]. The results obtained in the present work strongly support this argument. Since many number of chemical constituents are present in the onion juice, the question which supposed to be addressed is (i) which functional group is reduced by sulfur compounds and (ii) which one is reduced by NH_2 group?

Here, it is believed that the sulfur makes a C-S bond which is weaker compared to C-N bond. The sulfur atom may allow the de-epoxidation of GO more easily than NH_2 followed by the opening of the ring of epoxide [**28**]. In contrast, NH_2 group could also open the ring of epoxide and release water as by product. The NH_2 group may attack the sp^2-carbon nearest to the epoxide group from both the sides, resulting opening of the ring of the epoxide. Additionally, the C-C bond rotates the NH_2 group attached to the opposite side of the oxygen and bring NH_2 group close to the oxygen. The NH_2 group transfers one H-atom to the oxygen of epoxide and forms protonated groups. The other H-atom of NH_2 group transfers to the hydroxyl group (-OH), resulting the release of a water molecule [**31**]. However, the mechanism nevertheless requires more depth verification. It should be noted that the reaction temperature also influences the deoxygenation efficiency of the reducing agents [**32**].

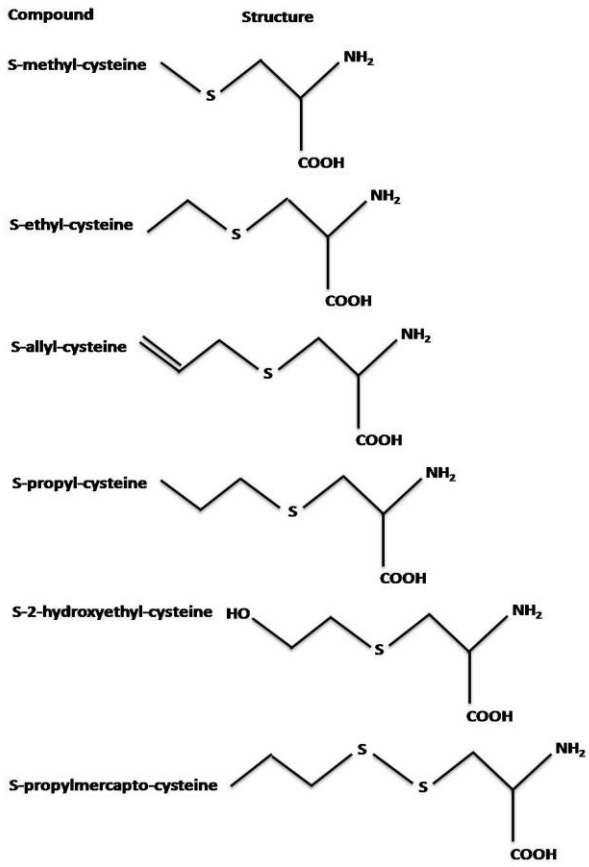

Fig. 2. Cysteine derivatives present in onion juice[21].

Structural and optical studies

XRD

The XRD patterns of GO, S1, S2, S3, S4 and S5, and S6 are shown in **Fig. 3.** It is reported that pristine graphite exhibits a diffraction peak at $2\theta=26.42^0$ (JCPDS No. 41-1487) corresponding to (002) plane with d-spacing of 0.336 nm [**33**]. Upon oxidation, it has been found that the (002) peak of pristine graphite shifts to the lower angle at $2\theta = 11.16^0$ corresponding to d-spacing of 0.87 nm which confirms the formation of GO. The increase in d-spacing is due to the attachment of oxygen containing functional groups and intercalation of water molecules to the layers of the graphite [**19**].

In contrast to GO, the rGO prepared at different concentrations of onion juice and heating temperature have different peak positions and d-spacing [**34**]. It is very clear from **Fig. 3** that the rGO prepared at room temperature using 0.5 and 1.5 ml of onion juice does not have prominent peak at (002) (generally exist at $24\text{-}26^0$) but shows peaks (100) at 41.17^0 and 41.37^0, respectively. While the rGO prepared at room temperature using 3, 5 and 10 ml of onion juice shows prominent peak (002) at

24.06^0, 24.69^0 and 25.2^0, respectively along with additional peaks at 43.29^0, 42.91^0 and 42.2^0, respectively. The sample S6 prepared at 65^0C using 3 ml of onion juice also shows prominent peak (002) as well as additional peaks (100) at 25.14^0 and 42.45^0, respectively. The value of d-spacing ~ 0.346 nm of S1, S2, S3, S4, S5 and S6 is close to that of the pristine graphite. The disappearance of peak at $2\theta=11.16^0$ indicates that the oxygen containing group of GO have been efficiently removed using onion juice as a reducing agent. The removing of oxygen containing functional groups with the recovery of a conjugated graphene like structure owing to partial reduction is the most attractive property of GO [**34**]. The significance of temperature on the reduction ability of onion juice could be visualized by looking at the XRD results. The quality of S6 is found to be better compared to samples synthesized at room temperature. Thus, it is believed that the recovery of a conjugated graphene like structure owing to partial reduction of GO could be achieved at certain reaction temperature by using specific concentration of the onion juice.

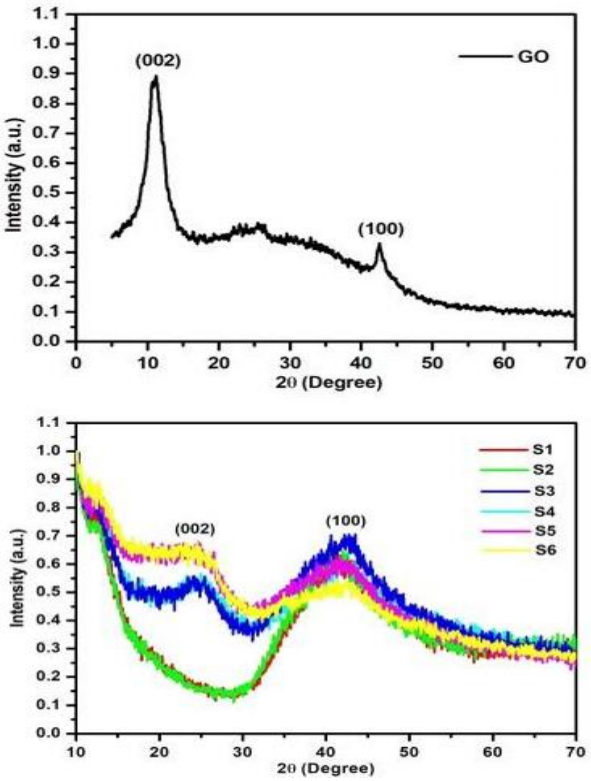

Fig. 3. XRD patterns of GO and rGO.

The increased d-spacing in the prepared rGO samples signifies the fact that NH_2 groups of onion juice could be covalently attached to the GO surface during reduction and layers are become well separated. The broadening of (002) peak in S5 and S6 compared to S3 and S4 indicating the formation of disordered stacking structures of few layer graphene. It indicates that the stacking structure of graphene layers could be reorganized with increasing onion juice concentration and heating temperature. It is expected that the π-π stacking interaction of rGO layers may result in a strong binding to the NH_2 molecules lying between them [**30**]. Recently, Liu *et al.*[**35**] has reported the direct redox reaction between the $–NH_2$ group of benzylamine and GO for reducing GO into rGO.

The number of graphene layers were calculated with the help of the Debye- Scherer equation demonstrated by Ju *et al.* [**36**]. The calculation yielded a variation in number of layers in rGO layers and the value is lying in the range 4–7, subjected to different reduction level depending upon the concentration of onion juice.

Raman spectroscopy

Raman spectroscopy is an important tool to study graphene and other carbon based materials. Fig. 4 shows the recorded Raman spectra of GO, S1, S2, S3, S4, S5 and S6 in the spectral range of 500-3000 cm^{-1}. The major Raman bands in graphite appears at 1334, 1575 and 2676 cm^{-1} assigned to D, G and 2D Raman bands, respectively. While in case of single layer graphene the D, G and 2D Raman bands positioned at ~1350, ~1580 and ~2690 cm^{-1}, respectively [**37**]. The G band arises from the first order scattering from the doubly degenerate E_{2g} phonon in-plane (sp^2 bonded carbons) vibrational modes of graphite in the Brillouin zone center as well as bond stretching of sp^2 carbon pairs in both, rings and chains. While, the D band occurs due to the breathing in-plane zone-edge mode of the k-point phonons of A_{1g} symmetry assigned to structural imperfections caused by the attachment of oxygenated groups on the carbon basal plane [**38, 39**]. Thus, the D band requires a defect for its activation and its intensity is therefore used to evaluate the degree of disorder. The intensity ratio of D to G band (ID/IG) represents a measure of disorder in graphene structure, which originates from defects associated with grain boundaries, vacancies and amorphous carbons [**40**]. Moreover, the overtone of the D band, called 2D band, is attributed to double resonance transitions resulting by the production of two phonons with opposite momentum. Furthermore, unlike the D peak, which is only Raman active in the presence of defects, the 2D peak is active even in the absence of any defects. The position and shape of 2D band is correlated with the number of layers present in the rGO [**38**].

In the Raman spectrum of GO, two noticeable fundamental vibrational bands named as the D band and the G band are observed at 1377 and 1627 cm^{-1}, respectively. The intensity of D band is comparable to that of the G band and the calculated I_D/I_G value for GO is about 1. It indicates the presence of significant structural disorder in the GO. It is worth to notice that in case of mechanically exfoliate perfect graphene, the D band is completely absent and the expected I_D/I_G value turns out to be 0. It means that the I_D/I_G value of rGO should be less than that of GO. As XRD results revealed that the quality of rGO is improved with increasing the concentration of onion juice, the I_D/I_G ratio of the

synthesized rGO must be reduced as the concentration of onion juice is increased. Therefore, Raman spectroscopy and XRD show a direct correlation between reduction level and growth in rGO.

The Raman spectra of rGO synthesized from onion juice assisted reduction of GO show two fundamental vibration bands observed in the range of 1300-1700 cm^{-1}. It is clear from **Fig. 4** that there is an apparent variation in Raman features like the peak positions of D and G bands and the value of I_D/I_G. It has also been noticed that the intensities of Raman peaks reduced gradually after reduction treatment, suggesting the different degrees of reduction of GO at various synthesis conditions. The position of Raman bands and the corresponding I_D/I_G ratio of all the samples are given in **Table 1**. By comparing the peak positions of D and G bands of the synthesized rGO, it is observed that as the concentration of onion juice and reaction temperature are increased, considerable red shift in the D and G bands was observed. Raman shift might be related to the stress generated in crystal lattice of rGO during its formation. During reduction, GO undergoes structural changes due to rearrangement of oxygen and carbon atoms. The shifting in position and change in I_D/I_G value of rGO compared to that of GO were employed to reveal the change in structure of synthesized rGO. It is reported that G band shifts to higher value side in case of well exfoliated graphene sheets while cutting graphene sheets leads to widening of the G band [**40, 41**]. Shi *et al.* [**42**] reported that the value of I_D/I_G may be used to know the degree of reduction. In the present study, it is observed that the value of I_D/I_G of rGO is gradually decreased with increasing the concentration of onion juice, indicating gradual improvement in sp^2 hybridized carbon atom structure. The value of I_D/I_G for all the synthesized rGO is found to be less than 1. It suggests the presence of more isolated graphene domain (sp^2 hybridized carbon atom structure) in the synthesized rGO. The in-plane sp^2 cluster size (L_A) can be calculated using the formula [**43**]:

$$L_A = 2.4 \times 10^{-10} \lambda^4 \left(\frac{ID}{IG}\right)^{-1}$$

where, λ denotes the wavelength of the laser light. There is an increase in the in-plane sp^2 cluster size (see **Table 1**) after increasing onion juice concentration and heating temperature. This is an indicative of the restoration of the sp^2 moieties after the reduction. The increase in the cluster size may be the outcome of alternation of C atoms from sp^3 to sp^2 bonded domains [**44**]. As, the I_D is proportional to the total number of defects (mostly come from sp^3 carbon) present in the synthesized samples, the decrease in the concentration of defects causes to increase the size of sp^2 clusters and ultimately the lattice gets distorted which influences the intensity of G band. Our results suggest that the lowering of I_D/I_G values may also be the consequence of the conversion of C atoms from sp^3 to sp^2. The defect density (n_D) in the rGO structure can be calculated using the relation [**43**]:

$$n_D{}^2 (cm^{-2}) = 7.3 \times 10^{-9} E_L{}^4 \left(\frac{ID}{IG}\right)$$

where, E_L denotes the energy of the laser light. A decrease of defect density is found from 2.26×10^{-7} cm^{-2} to 0.96×10^{-7} cm^{-2} after different reduction of GO into rGO.

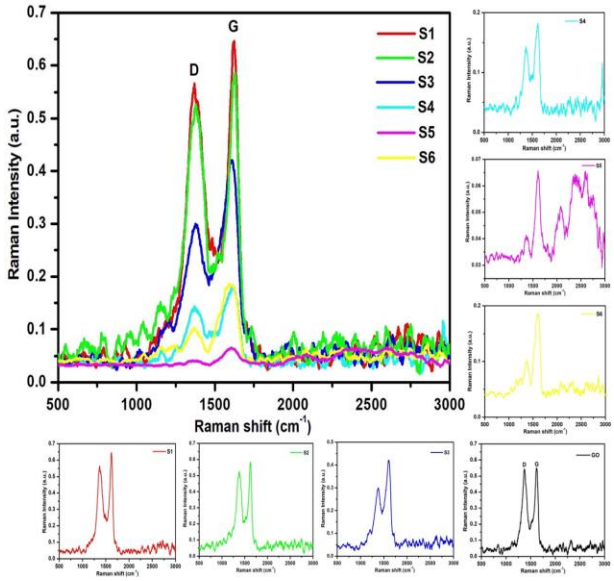

Fig. 4. Raman spectra of GO and rGO.

Table 1. The D, G, I_D/I_G, in-plane sp^2 cluster size (L_A) and defect density (n_D) of the synthesized GO and rGO samples.

Sample	D (cm^{-1})	G (cm^{-1})	I_D/I_G	In-plane sp^2 cluster size (L_A) nm	Defect density (n_D) cm^{-2}
S1	1377	1623	0.92	18.20	2.26×10^{-7}
S2	1376	1621	0.88	19.03	2.16×10^{-7}
S3	1370	1614	0.77	21.75	1.89×10^{-7}
S4	1368	1606	0.7	23.93	1.72×10^{-7}
S5	1357	1605	0.39	42.95	0.96×10^{-7}
S6	1348	1590	0.5	33.50	1.23×10^{-7}
GO	1377	1627	0.99	16.92	2.43×10^{-7}

The effect of change in the synthesis temperature from room temperature to 65° C for a definite concentration (3ml) of onion juice has been studied considering the peak position and ID/IG vale of S3 and S6. The position Raman peaks in S6 is red shifted compared to that of S3. The value of I_D/I_G in S6 is decreased compared to that of S3, suggesting the degree of disorder in the graphene structure, which may be due to the increase in synthesis temperature. It is believed that the increase in reaction temperature could develop anharmonic coupling of phonons and boost the thermal expansion in the lattice, resulting in shift of G band towards lower wavenumber side. In the present case, the width of the G band remained unchanged up to the addition of 1.5ml of onion juice at room temperature while the D band intensity is varied followed by a slight change in the width of G band starts at the 3ml concentration of onion juice. The lack of broadening in

the G band supports that the D band originates from the edges. Even though the defect peak is observed in all the samples, we suggest that after adding 3ml of onion juice at room temperature as well as at higher temperature, the D band not only comes from edges of the graphene sheets but also from structural defects inside the graphene plane.

The 2D Raman band is the characteristic of double resonance transitions resulting from two-phonon Raman scattering process with opposite momentum (+k and -k) [**45**]. The 2D peak intensity in GO and rGO is found weak and careful data acquisition is necessary to study its characteristics. However, the features of 2D peak were observed only in case of S5. The Gaussian peak fitting of 2D band reveals four peaks at ~2505, ~2609, ~2740 and ~2786 cm^{-1}. It is well known that the appearance of 2D Raman band is important to estimate the number of layers in the rGO [**46**]. The S5 sample shows intense 2D peak, indicating less disorder in its structure. This may be due to the extremely fast process to get less time to form disordered lattice structure. Generally, the 2D Raman band of the monolayer graphene is observed at ~2679 cm^{-1} and this peak shifts to higher wavenumber (blue shift) side in case of multi-layer graphene. It suggests the stronger interlayer coupling accompanied by removal of trapped interlayer species and functional groups [**47**]. In multi-layer stacked graphene, the 2D peak splits into two major and two minor components due to coupling between the layers [**37**]. The 2D-peak splitting in rGO spectra has been reported but it is often absent, probably due to weak interlayer coupling it has been observed in the present case in most of the rGO samples. On the other hand, the I_{2D}/I_G ratios of single, double, triple and multi-layer graphene sheets are reported to be >1.6, ~0.8, ~0.30 and ~0.07, respectively [**48**]. In the present investigation, the 2D band is observed in S5 sample with I_{2D}/I_G value ~ 0.87. Unlike D and G bands, the changes in 2D bands were not distinct in the samples other than S5. This result indicates that the synthesized S5 sample may have more than two layers.

TEM

The TEM images of the synthesized S5 and S6 are shown in **Fig. 5a-b**. It shows a silky appearance with very less wrinkles and the planes overlap on each other. The transparent and silky nature of rGO confirms its stability under high energy electron beam [**19**]. From **Fig. 5**, it is cleared that the synthesized rGO is very thin and consisting of few layers. It is consistent with results obtained by Raman measurements. The SAED pattern as shown in the inset of **Fig. 5** reveals the presence of all the diffraction rings which further support the formation of few layer graphene. The observation of some sharp diffraction spots in the SAED pattern of S6 indicate the presence of disorder which is also well supported by the presence of D band in the Raman spectrum. The interlayer distance calculated from TEM images is in good agreement with the XRD result.

Wrinkles and overlaps are two elementary morphological features of graphene materials [**49**]. Cote *et al*. [**50**] studied that these wrinkles and overlaps greatly depend on the pH of the solution. They have observed that graphene sheets became much more hydrophilic under basic conditions while hydrophobic under acidic. The presence of water molecule within the layers of graphene provide favorable conditions for the overlapped morphology. Due to the hydrophilic nature, graphene sheets intercalated with water molecules provide favorable conditions for sliding the sheets upon each other and gives an overlapped morphology. On the other hand, in acidic media, the edges of the interacting sheet are fixed due to hydrogen bonding between the carboxylic acid edge groups and prevent these sheets from sliding, resulting in wrinkles over the surface. Shen *et al*. [**51**] has also suggested that the wrinkles and crumpled graphene sheets can be formed because of the increased surface tension in the water casting process. The structure and morphology of graphene are also affected by the degree of oxidation, reduction, thickness, and relative concentration of hydroxyl (-OH) and epoxide (-O-) functional groups. It has been found that increased coverage of hydroxyl groups makes graphene to act as a brittle material, whereas epoxide groups strengthen the ductile nature of GO [**52**]. Likewise, Liu and Wang [**53**] reported that the formation of wrinkles is ascribed as defects in the carbon structure due to a long-range stress developed on the graphene surface due to adsorbed additional atoms.

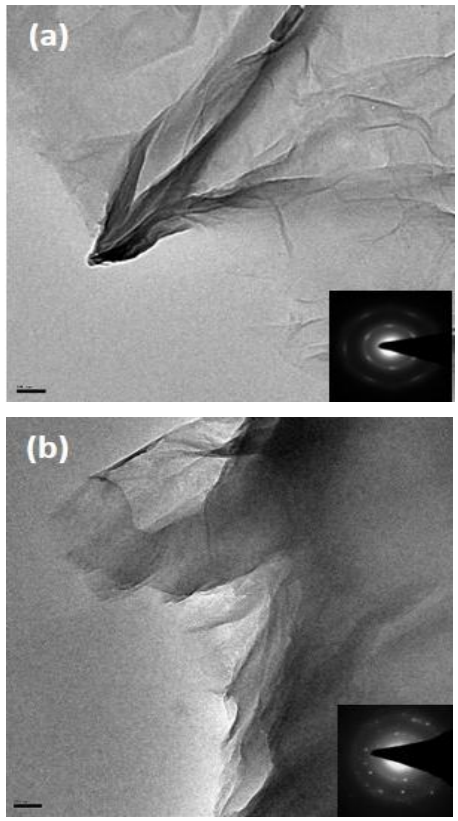

Fig. 5. TEM images (a-b) of S5 and S6, respectively. Inset of Fig. 5 (a-b): SAED pattern.

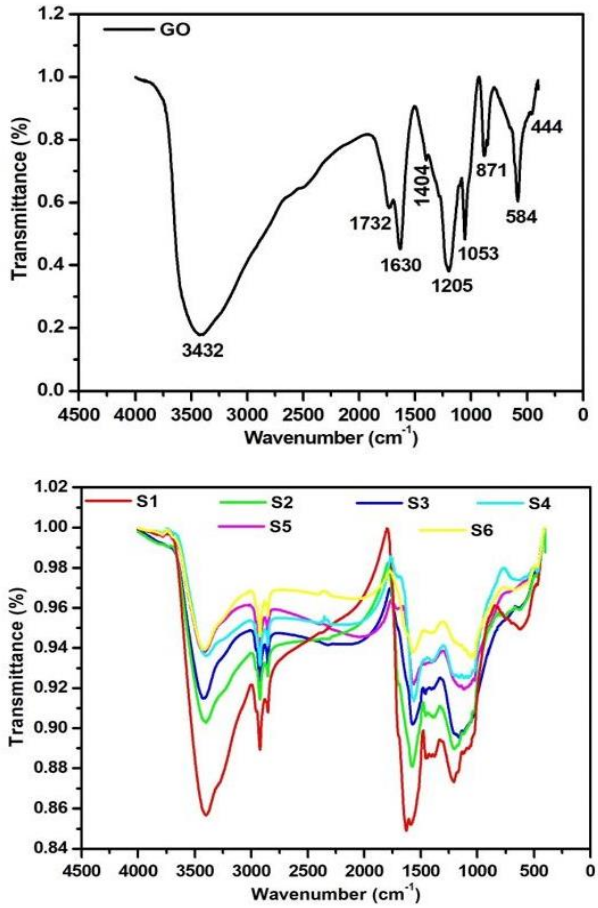

Fig. 6. FTIR spectra of GO and rGO.

FTIR

The FTIR spectra of the synthesized rGO samples are shown **Fig. 6**. Generally, four kinds of oxygen containing functional groups such as; epoxide (-O-), hydroxyl (-OH), carbonyl (-C=O) and carboxyl (-COOH) are known to exist in the GO. The epoxide and hydroxyl functionalities are major components located on the basal plane of GO while carbonyl and carboxyl are minor oxygen functionalities distributed at the edges of GO [**19**]. The presence of oxygen containing groups in the synthesized samples is clearly confirmed by looking at the FTIR spectra (see **Fig. 6**). In the FTIR spectra of GO, the peaks at ~3432 cm^{-1} and ~1404 cm^{-1} correspond to O–H stretching and deformation vibration, respectively, while the peak positioned at ~1732 and ~1630 cm^{-1} are assigned to C=O stretching vibration and aromatic C=C stretching vibration, respectively. The peak at ~1205 and ~1053 cm^{-1} can be ascribed to the stretching vibrations of C–O of epoxy and alkoxy C–O stretching vibration mode, respectively [**54**]. The appearance of a low intense peak at ~2350 cm^{-1} is associated with carbon dioxide [**17**]. Likewise, the peak at ~871 corresponds to aromatic C-H deformation [**55**]. The peaks at ~584 and ~444 cm^{-1} are referred to the characteristics of the epoxy stretching mode located over the basal plane of the GO [**56, 57**] and ether [**48**] respectively. The existence of these oxygen functionalities in GO confirms the hydrophilicity and stability of GO in aqueous systems.

The FTIR spectra of rGO synthesized at various concentrations and reaction temperatures show the peaks in the spectral range of 3431-3402 cm^{-1}. These peaks mainly attributed to the stretching vibrations of O-H bonds. Two additional weak bands were observed in the spectral range 2922-2924 and 2852-2853 cm^{-1}. These bands were absent in the FTIR spectra of GO. The bands are assigned to C-H stretching mode and N–H bending mode of the amine group [**57**]. The peak in S1 correspond to carbonyl (C = O) groups at 1709 cm^{-1}. This peak is absent in the other samples. The peak at ~1627 cm^{-1} in S1 is assigned to C=C stretching. This peak is appeared at different wavenumber positions in the FTIR spectra of other samples. The peaks at ~1388 cm^{-1} and 1376 cm^{-1} present in the FTIR spectra of S4 and S5, respectively correspond to C−O stretching mode [**40**], which indicating the hydrophilic nature of rGO. However, it was not present in the other samples prepared at lower concentration of onion juice. The disappearance of FTIR band associated with the various oxygen containing functional groups clearly validates the strong reducing ability of onion juice to transform GO into rGO.

UV-Vis. spectroscopy

The reduction phenomenon was also monitored by recording the UV-Vis. absorption spectra of the rGO samples synthesized at different conditions. The reduction of GO through onion juice could clearly be seen by changing the brown color of the aqueous dispersion of GO into black color of rGO as shown in the inset of **Fig. 7**. The UV–Vis. absorption spectrum of GO shows the plasmonic peak at ~232 nm due to π–π* transition of aromatic C=C bonds in sp^2 hybridization region and a shoulder peak at ~303 nm, assigned to n–π* transitions of C=O bonds [**58**]. While in case of rGO, the plasmon peak shifted to higher wavelength side and appeared at ~ 275 nm for the samples synthesized at higher concentrations. It may be due to the increased π-electron concentration and structural ordering through the restoration of sp^2 carbon network [**5**]. It implies that the GO is reduced effectively using onion juice. This result is consistent with the results obtained from XRD, Raman and FTIR measurements. The UV-Vis results indicate the higher oxygen content at lower concentration of onion juice as well as lower reaction temperature. The sharpness and absorbance of absorption peak corresponding to π-π* transition are increased gradually with increasing the concentration of onion juice. The electronegative oxygen functional groups disrupt the π-network symmetry and it is believed that after partial reduction, the rGO becomes a mixture of sp^2 and sp^3 carbon domains where sp^2 carbon atoms are linked to the neighboring carbon atoms while the sp^3 carbon atoms are joined to the adjacent oxygen-containing functional groups. Thus, the electronic structure of rGO is depended on the atomic ratio of

sp^2/sp^3 hybridized carbon atoms [**48**]. In such cases, the interaction between π and oxygen-related electronic states make π states to disappear near the Fermi level [**59**]. Therefore, the observed behavior of obtained absorption spectra in the present study reflects that the change in onion juice concentration as well as reaction temperature would influence the structure and optical behavior of the rGO. The red shifting of π–π* transition of rGO (prepared with different concentrations of onion juice) compared to GO suggests that the contribution of aromatic sp^2 domains are increased owing to increasing the degree of reduction [**58**]. It has been demonstrated by Cushing *et al.* [**60**] that the strength of π-π* transition peaks is attributed to the presence of -OH functional group in the samples. The absorption spectra reveal that the number of -OH functional groups are increased with increasing the concentration of onion juice and reaction temperature which ultimately leads to the tunable optical properties of rGO that could be useful for various applications.

To examine the aqueous dispersion stability of the prepared rGO sample, the samples were dispersed in distilled water at a typical concentration of 0.5 mg/ml followed by ultrasonication at room temperature. The digital image of aqueous dispersion of S5 and S6 samples are shown in the inset of **Fig. 7**. The prepared rGO is well dispersed in the distilled water as evidenced by the existence of black homogeneous solution. The present results suggest that the aqueous suspension of onion juice assisted synthesized rGO could be prepared in distilled water for various practical applications.

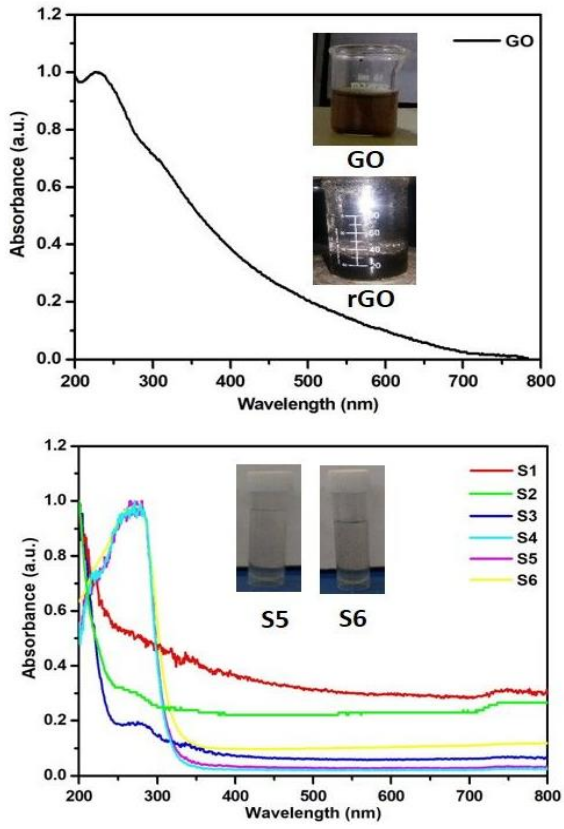

Fig. 7. UV-Vis. spectra of GO and rGO.

Conclusion

The use of toxic reducing agents for the chemical reduction of GO into are harmful to human health and environment. The complicated surface modification during chemical reduction process is often needed to avoid aggregation of rGO. Here, we have reported a green and facile method for the synthesis of rGO based on the reduction of exfoliated GO using onion juice. The most important advantages of the onion juice are their abundance in nature and cost effectiveness. This green method could be applicable for large scale production of rGO. The reduction process was carried out in aqueous medium at a specific temperature. We demonstrated that the onion juice has tremendous potential to be used as reducing agent for the reduction of GO. The XRD, UV-Vis. and FTIR measurements of the resultant rGO powder samples confirm the high reduction ability of onion juice. The TEM measurements reveal the formation of silky and wrinkled graphene layers. The Raman spectra were used to assess the quality of the synthesized rGO materials. The obtained features of aqueous dispersibility endow this green approach to construct various rGO based materials with great potential. The main advantages of this approach over the conventional chemical reduction are the cost-effectiveness, environmental friendly and simple reduction process to produce graphene like configuration with unique in structural and optical properties.

Acknowledgement

SK is thankful to University Grants Commission, India for providing financial support through D. S. Kothari Postdoctoral Fellowship Scheme (No.F.4-2/2006(BSR)/PH/15-16/0067).

References

1. Allen, M. J.; Tung, V. C.; Kaner, R. B., *Chem. Rev.*, **2010**, *110*, 132.
2. Novoselov, K. S.; Geim, A. K.; Morozov, S. V.; Jiang, D.; Zhang, Y.; Dubonos, S. V.; Grigorieva, I. V.; Firsov, A. A., *Science*, **2004**, *306*, 666.
3. Wang, G.; Shen, X.; Yao, J.; Park, J., *Carbon*, **2009**, *47*, 2049.
4. Fowler, J. D.; Allen, M. J.; Tung, V. C.; Yang, Y.; Kaner, R. B.; Weiller, B. H., *ACS Nano*, **2009**, *3*, 301.
5. Kumar, S.; Ojha, A. K.; Ahmed, B.; Kumar, A.; Das, J.; Materny, A., *Materials Today Communications*, **2017**, *11*, 76.
6. Park, S.; An, J.; Potts, J. R.; Velamakanni, A.; Murali S.; Ruoff, R. S., *Carbon*, **2011**, *49*, 3019.
7. Kim, N. H.; Kuila T.; Lee, J. H., *J. Mater. Chem. A*, **2013**, *1*, 1349.
8. Wang, G.; Yang, J.; Park, J.; Gou, X.; Wang, B.; Liu H.; Yao, J., *J. Phys. Chem. C*, **2008**, *112*, 8192.
9. Shin, H. J.; Kim, K. K.; Benayad, A.; Yoon, S. M.; Park, H. K.; Jung, I. S.; Jin, M. H.; Jeong, H. K.; Kim, J. M.; Choi, J. Y.; Lee, Y. H., *Adv. Funct. Mater.*, **2009**, *19*, 1987.
10. Wang, Y.; Shi, Z. X.; Yin, J., *ACS Appl. Mater. Interfaces*, **2011**, *3*, 1127.
11. Kuila, T.; Bose, S.; Khanra, P.; Mishra, A. K.; Kim N. H.; Lee, J. H., *Carbon*, **2012**, ***50***, 914.
12. Zheng, Y.; Wang, A.; Cai, W.; Wang, Z.; Peng, F.; Liu, Z.; Fua, L., *Enzyme Microb. Technol.*, **2016**, *95*, 112.
13. Gao, J.; Lui, F.; Lui, Y.; Ma, N.; Wang, Z.; Zhang, X., *Chem. Mater.*, **2010**, *22*, 2213.
14. Zhu, C.; Guo, S.; Fang, Y.; Dong, S., *ACS Nano*, **2010**, 4, 2429.
15. Akhavan, O.; Ghaderi, E.; Aghayee, S.; Fereydooni, Y.; Talebi, A., *J. Mater. Chem.*, **2012**, *22*, 13773.

16. Peng, H. D.; Meng, L. J.; Niu, L. Y.; Lu, Q. H., *J. Phys. Chem. C*, **2012**, *116*, 16294.
17. Chong, S. W.; Lai, C. W.; Abdul Hamid, S. B., *Ceram. Int.*, **2015**, *41*, 9505.
18. Salas, E. C.; Sun, Z.; Luttge, A.; Tour, J. M., *ACS Nano*, **2010**, *4*, 4852.
19. Kumar, S.; Kumar, A., *Opt. Mater.*, **2016**, *62*, 320.
20. Marcano, D. C.; Kosynkin, D. V.; Berlin, J. M.; Sinitskii, A.; Sun, Z.; Slesarev, A.; Alemany, L. B.; Lu, W.; Tour, J. M., *ACS Nano*, **2010**, *4*, 4806.
21. Dini, I.; Tenore, G. C.; Dini, A., *Food Chem.*, **2008**, *107*, 613.
22. Chen, D.; Li, L.; Guo, L., *Nanotechnology*, **2011**, *22*, 325601.
23. Wang, J.; Salihi, E. C.; ŠillerIn, L., *Mater. Sci. Eng., C*, **2017**, *72*, 1
24. Ma, J.; Wang, X.; Liu, Y.; Wu, T.; Liu, Y.; Guo, Y.; Ruqiang, L.; Sun, X.; Wu, F.; Li, C.; Gao, J., *J. Mater. Chem. A*, **2013**, *1*, 2192.
25. Xu, X.; Wu, T.; Xia, F.; Li, Y.; Zhang, C.; Zhang, L.; Chen, M.; Li, X.; Zhang, L.; Liu, Y.; Gao, J., *J. Power Sources*, **2014**, *266*, 282.
26. Sarkar, S.; Basak, D., *Chem. Phys. Lett.*, **2013**, *561*, 125.
27. Li, X.; Xu, X.; Xia, F.; Bu, L.; Qiu, H.; Chen, M.; Zhang, L.; Gao, J., *Electrochim. Acta*, **2014**, *130*, 305.
28. Chen, W.; Yan, L.; Bangal, P. R., *J. Phys. Chem. C*, **2010**, *114*, 19885.
29. Jin, S. H.; Kim, D. H.; Jun, G. H.; Hong, S. H.; Jeon, S., *ACS Nano*, **2013**, *7*, 1239.
30. Navaee, A.; Salimi, A., *RSC Adv.*, **2015**, *5*, 59874.
31. Gao, X.; Jang, J.; Nagase, S., *J. Phys. Chem. C*, **2010**, *114*, 832.
32. Yang, D.; Velamakanni, A.; Bozoklu, G.; Park, S.; Stoller, M.; Piner, R. D.; Stankovich, S.; Jung, I.; Field, D. A.; Jr. Ventrice, C. A.; Ruoff, R. S., *Carbon* **2009**, *47*, 145.
33. Kumar, S.; Ojha, A. K., *Mater. Chem. Phys.*, **2016**, *171*, 126.
34. Kumar, S.; Ojha, A. K.; Walkenfort, B., *J. Photochem. Photobiol. B, Biol.*, **2016**, *159*, 111.
35. Liu, S.; Tian, J.; Wang, L.; Sun, X., *Carbon*, **2011**, *49*, 3158.
36. Ju, H. M.; Huh, S. H.; Choi, S. H.; Lee, H. L., *Mater. Lett.*, **2010**, *64*, 357.
37. Gayathri, S.; Jayabal, P.; Kottaisamy, M.; Ramakrishnan, V., *AIP Adv.*, **2014**, *4*, 027116.
38. Ferrari, A.; Robertson, J., *Phys. Rev. B*, **2000**, *61*, 14095.
39. Jain, R.; Mishra, S., *RSC Adv.*, **2016**, *6*, 27404.
40. Bayat, A.; Saievar-Iranizad, E., *J. Lumin.*, **2017**, *192*, 180.
41. Krishnamoorthy, K.; Veerapandian, M.; Mohan, R.; Kim, S. J., *Appl. Phys. A*, **2012**, *106*, 501.
42. Shi, G.; Meng, Q.; Zhao, Z.; Kuan, H. C.; Michelmore, A.; Ma, J., *ACS Appl. Mater. Interfaces*, **2015**, 7, 13745.
43. Ferrari, A. C.; Meyer, J. C.; Scardaci, V.; Casiraghi, C.; Lazzeri, M.; Mauri, F.; Piscanec, S.; Jiang, D.; Novoselov, K. S.; Roth, S.; Geim, A. K., *Phys. Rev. Lett.*, **2006**, *97*, 187401.
44. Jovanovic, S. P.; Markovic, Z. M.; Syrgiannis, Z.; Dramicanin, M. D.; Arcudi, F.; Parola, V. L.; Budimir, M. D.; Markovic, B. M. T., *Mater. Res. Bull.*, **2017**, *93*, 183.
45. Malard, L. M.; Pimenta, M. A.; Dresselhaus, G.; Dresselhaus, M. S., *Physics Reports*, **2009**, *473*, 51.
46. Ferrari, A. C., *Solid State Commun.*, **2007**, *143*, 47.
47. Graf, D.; Molitor, F.; Ensslin, K.; Stampfer, C.; Jungen, A.; Hierold, C.; Wirtz, L., *Nano Lett.*, **2007**, *7*, 238.
48. Kumar, S.; Baruah, B.; Kumar, A., *Materials Today Communications*, **2017**, *13*, 26.
49. Sajjad, S.; Khan Leghari, S. A.; Iqbal, A., *ACS Appl. Mater. Interfaces*, **2017**, *9*, 43393.
50. Cote, L. J.; Kim, J.; Zhang, Z.; Sun, C.; Huang, J., *Soft Matter*, **2010**, *6*, 6096.
51. Shen, X.; Lin, X.; Yousefi, N.; Jia, J.; Kim, J. K., *Carbon*, **2014**, *66*, 84.
52. Soler-Crespo, R. A.; Gao, W.; Xiao, P.; Wei, X.; Paci, J. T.; Henkelman, G.; Espinosa, H. D., *J. Phys. Chem. Lett.*, **2016**, *7*, 2702.
53. Wang, F.; Liu, J., *Nanoscale*, **2015**, **7**, 919.
54. Lou, Q.; Ji, W. Y.; Zhao, J. L.; Shan, C. X., *Nanotechnology*, **2016**, *27*, 325201.
55. Wang, Z.; Huang, B.; Dai, Y.; Liu, Y.; Zhang, X.; Qin, X.; Wang, J.; Zheng, Z.; Cheng, H., *CrystEngComm*, **2012**, *14*, 1687.
56. Guerrero-Contreras, J.; Caballero-Briones, F., *Mater. Chem. Phys.*, **2015**, *153*, 209.
57. Kumar, S.; Kumar, A., *Mater. Sci. Eng., B*, **2017**, *223*, 98.
58. Paredes, J. I.; Villar-Rodil, S.; Martinez-Alonso, A.; Tascon, J. M. D., *Langmuir*, **2008**, *24*, 10560.
59. Yan, J.; Xian, L.; Chou, M. Y., *Phys. Rev. Lett.*, **2009**, *103*, 086802.
60. Cushing, S. K.; Li, M.; Huang, F.; Wu, N., *ACS Nano*, **2014**, *8*, 1002.

